Energy Education Science and Technology Part A: Energy Science and Research
2010 Volume (issue) **24(2):** 151-171

A mathematical model for condensation of bubbles injected through an orifice into subcooled water

A. Bugutekin[1*], M. Yilmaz[2], A. Kentli[3], M. O. Isikan[4]

[1]Adiyaman University Vocational High School Gölbaşı Karayolu 02040 Adıyaman– Turkey,
Tel.: 0416-2212325–26-27 Fax: 0416-2232129 Email: abugutekin@adiyaman.edu.tr
[2,3] Marmara University Faculty of Engineering Kuyubaşı/Istanbul – Turkey
[4]Marmara University Faculty of Technical Education Kuyubaşı/Istanbul – Turkey

Received: 15 August 2009; accepted: 07 September 2009:

Abstract

In this investigation, a semi-empirical equation is developed to predict the collapse rate of steam bubbles injected through an orifice into subcooled water. The equation considers both bubble distortion and the heating of the liquid around the condensing bubble. The theoretical predictions correlate experimental data reasonably well.

Keywords: Cooling; Condensation; Mathematical modeling
© Sila Science. All rights reserved

1. Introduction

The processes governing the growth or collapse of vapor bubbles in a liquid pool are determined mainly by the temperature of the liquid and by interactions resulting from hydrodynamic behavior of the bubbles in the liquid pool. The precise effects of these parameters can involve both heat transfer between bubble and liquid and liquid inertia. In some cases liquid inertia may be the dominant feature while in others heat transfer may be main factor controlling growth or collapse. Many research workers, using an extended form of the Rayleigh equation, originally developed for the collapse of a cavity in a liquid, have demonstrated the close relationship between the phenomena of bubble growth and those of bubble collapse.

* Corresponding author. Tel.: +90-416-223-2125; fax: +9- 416-223-2129.
E-mail address: abugutekin@adiyaman.edu.tr (A. Bugutekin).

This, of course, implies that many of the features noted by these workers in bubble growth may also be important factors in the field of bubble collapse. Bankoff has given an extensive review of heat transfer controlled bubble growth [1]. An extensive amount of work has been carried out into the growth of vapor bubbles in a superheated liquid and much of this has been the subject of a comprehensive review in a book on boiling phenomena by Van Stralen and Cole [2]. A comprehensive review on direct contact heat transfer was given in the reference [3]. In addition, an experimental investigation of the dynamics of, and the heat transfer to, the vapor bubbles condensing in subcooled liquid was performed by Kalman and Mori [4].

There are a few amounts of experimental data and theoretical study on vapor bubbles condensing in subcooled liquids. Nucleation and bubble formation are well understood and frequently studied in the literature. In contrast to this, much less known about the parameters controlling the collapse in spite of fact that bubble condensation was already studied in the literature.

Less of the existing quasi-steady state theories take into account of radial velocities, bubble distortion or local temperature differences produced around the condensing bubbles. Each of these may have some effect on the collapse rate of the bubble although the relative magnitude of the different effects should depend on the parameters controlling the collapse. For example, radial velocities may be comparable with the bubble rise velocity especially at high subcoolings, there may be bubble distortion especially early in the collapse and the condensation of the bubble may lead to local heating of the water around the bubble.

Ruckenstein and Davis presented a general solution for a growing bubble, with allowance made for radial velocity effects but with no allowance made for either distortion or local temperature changes [5]. This gave the bubble radius R at any time t in terms of a complicated integral equation, which was solved iteratively for certain cases of the growth of vapor bubbles, but the result is found to be too complicated for ready engineering use.

It would therefore be desirable to obtain a reasonable solution, easier to use, and including the effects of the three variables mentioned.

2. Experimental apparatus

A sketch of bubble chamber test rig is shown in Fig. 1, the main components being a steam boiler, a steam flow measuring section and a bubble test chamber incorporating an injection orifice or nozzle. Details are given in [2]. The bubble test chamber is 180 mm^2 and 240 mm high with glass windows on three sides to permit high speed photography of the condensation process. The chamber can be filled to any desired level and can be operated up to a pressure of 4 bars.

A shadow-graph optical system was used to record the growth and collapse of the steam bubbles. Such experiments were performed with more extensive or accurate measurement systems [6] but it is seen that results are enough accurate. The camera was a Hitachi 16 mm high speed cine camera and a DT – 11A HIPAD digitizer, interfaced to a computer, was used to obtain measured values of bubble volume, bubble surface area and bubble position at a series of times from the start of bubble growth throughout both growth and collapse periods.

3. Experimental conditions

Details of the procedure are given in [2]. Three bubbles are analyzed at each condition. The range of test conditions covered is as follows (test results will be given in detail at the following sections):

Steam flow rates: 3 steps ranging from 0.5 to 1.5 g/min
Sub-cooling : at 1 bar range from 5 K to 29.7 K to give Jakob number of 15, 30, 45, 60, and 75 and at 2 bar range from 9.3 K to 36.6 K to give Jakob numbers 15, 30, 45, and 60.
Pressures : 1 and 2 bar
Orifice Diameters: 1 mm and 2 mm

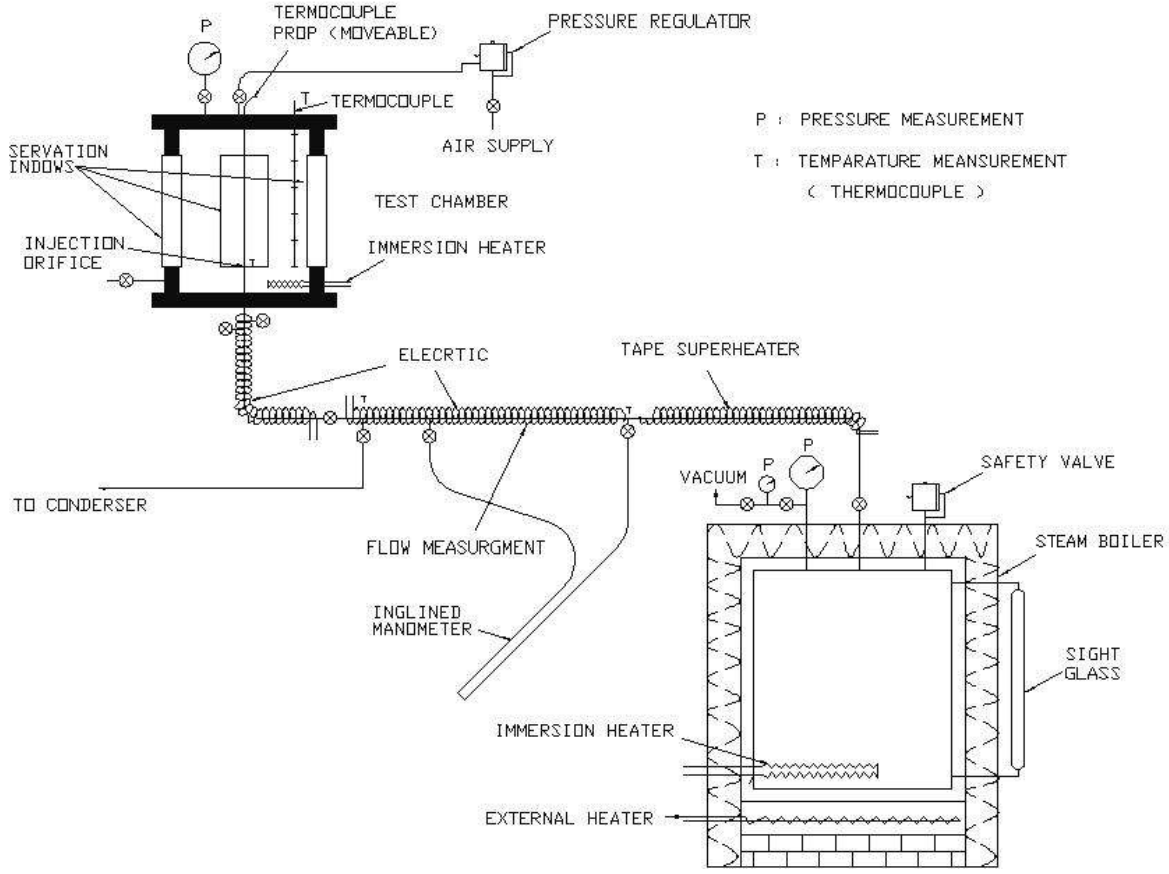


Fig. 1. Layout of steam bubble condensation rig.

4. Theory

A simplified approximate solution is presented below, allowing for radial velocities in addition to the velocities due to the vertical motion of the bubbles. Before focusing the subject, it should be phrased that many approximations and assumptions are taken into account because analytical modeling is concerned in this study. Many works using fewer assumptions to model the same system could be found in literature, but, most of them are either numerically modeled or giving less accurate results according our approach.

The convection of heat in the water flowing around a spherical bubble is assumed to be given, in spherical coordinates, by the energy equation as

$$\frac{\partial T}{\partial t} + u_r \frac{\partial T}{\partial r} + \frac{u_\theta}{r} \frac{\partial T}{\partial \theta} = \alpha \left(\frac{\partial^2 T}{\partial r^2} + \frac{2}{r} \frac{\partial T}{\partial r} \right) \tag{1}$$

where t (time) in s, u_r (velocity in the radial direction) in m/s, u_θ (velocity in the tangential direction) in m/s, α (thermal diffusivity) in m^2/s. Conduction in the tangential direction is assumed to be much smaller than in the radial direction, and hence is neglected. Viscous dissipation is also neglected because flow around the bubble is assumed to be inviscid.

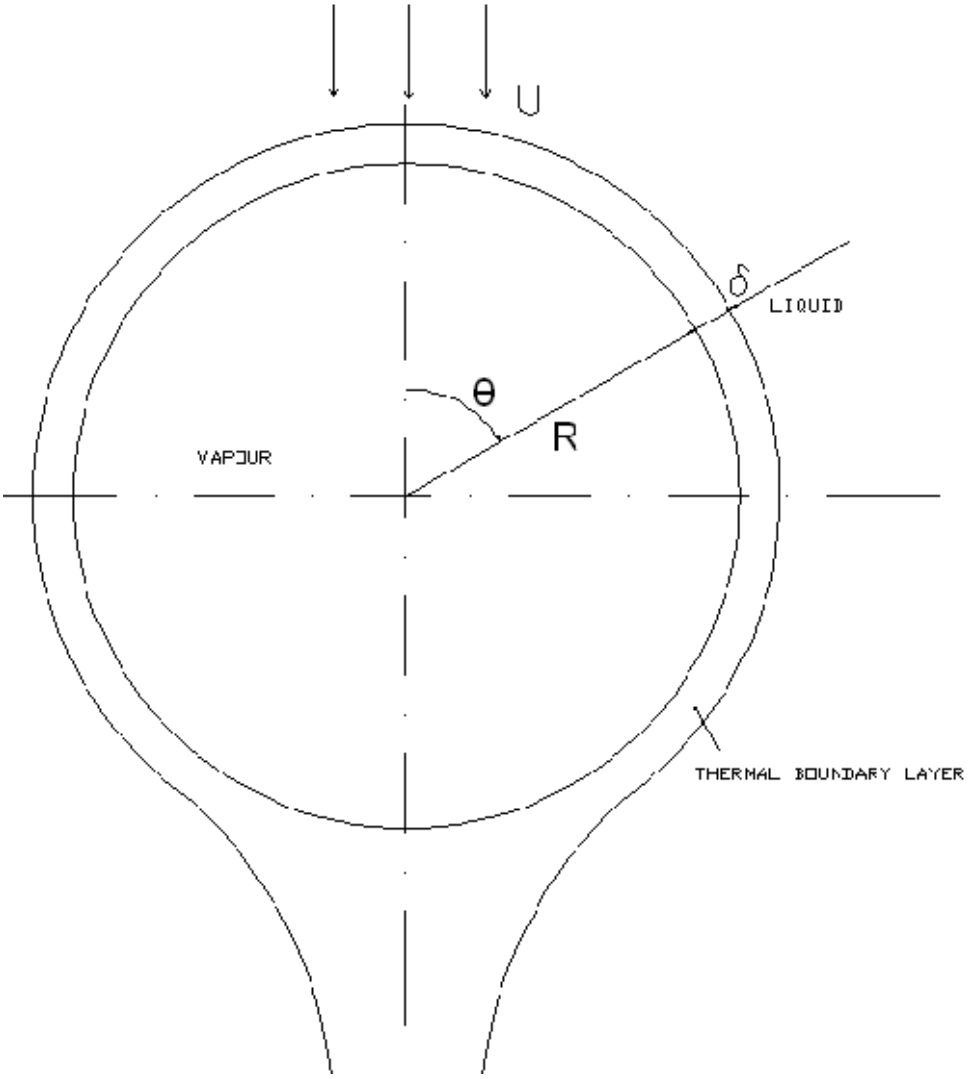


Fig. 2. Theoretical bubble collapse model

Assumptions:

- Bubble is spherical (illustrated in Fig. 2)
- $\frac{\partial^2 T}{\partial r^2} = \frac{2}{r}\frac{\partial T}{\partial r}$ ($\frac{2}{\mathrm{r}}\frac{\partial \mathrm{T}}{\partial \mathrm{r}}$ is neglected)
- Conduction in the tangential direction(neglected) is much smaller than in the radial direction
- Bubble is in viscid (viscous dissipation is neglected)
- Simplified potential flow around bubble and thickness of thermal boundary layer is small
- $\frac{y}{R} = 1$ while y = r – R (second or higher order terms are neglected)
- Bubble is rising in a vertical path with a constant velocity, U [7-12]

Assuming simplified potential flow around the bubble and that the thickness of the thermal boundary layer is small, the velocities in the radial direction, u_r and in the tangential direction u_θ are given as

$$u_r = -U\left[1-\left(\frac{R}{r}\right)^3\right]\cos\theta + \dot{R}\frac{R^2}{r^2} \tag{2}$$

$$u_\theta = U\left[1+\frac{1}{2}\left(\frac{R}{r}\right)^3\right]\sin\theta \tag{3}$$

Changing the coordinate system to a moving coordinate, y = r – R and neglecting second or higher order terms since $\frac{y}{R} \langle\langle 1$

$$u_r \cong -2U\frac{y}{R}\cos\theta + \dot{R}\left(1-2\frac{y}{R}\right) \tag{4}$$

$$u_\theta = \frac{3}{2}U\sin\theta \tag{5}$$

Returning to the Eq. (1), $\frac{\partial^2 T}{\partial r^2} \approx \frac{T}{y^2}$ and $\frac{2}{r}\frac{\partial T}{\partial r} \approx \frac{2}{r}\frac{T}{y}$

Hence $\frac{\partial^2 T}{\partial r^2} = \frac{2}{r}\frac{\partial T}{\partial r}$, and the term $\frac{2}{\mathrm{r}}\frac{\partial \mathrm{T}}{\partial \mathrm{r}}$ can be neglected.

In moving coordinate system, $\left(\frac{\partial T}{\partial t}\right)_{r,\theta} \equiv \left(\frac{\partial T}{\partial t}\right)_{y,\theta} - \dot{R}\left(\frac{\partial T}{\partial y}\right)$ and $\frac{\partial T}{\partial r} \equiv \frac{\partial T}{\partial y}$

Thus Eq. (1) becomes,

$$\frac{\partial T}{\partial t} - \frac{y}{R}\left[3U\cos\theta + 2\dot{R}\right]\frac{\partial T}{\partial y} + \frac{3}{2}\frac{U}{R}\sin\theta\frac{\partial T}{\partial \theta} = \alpha\frac{\partial^2 T}{\partial y^2} \tag{6}$$

which is the Eq. (9) of Ruckenstein and Davis [5] where $\dot{R}$ (Bubble wall radial velocity, dR/dt) in m/s, θ (polar angle from vertical) in rad.

If it is now further assumed that $\frac{\partial T}{\partial t} = \frac{y}{R}\dot{R}\frac{\partial T}{\partial y}$ and if Eq. (6) is integrated across the thermal boundary layer thickness δ(θ),

$$\alpha\int_0^{\delta}\frac{\partial^2\phi}{\partial y^2}dy = -\left(3\frac{U}{R}\cos\theta + 2\frac{\dot{R}}{R}\right)\int_0^{\delta} y\frac{\partial\phi}{\partial y}dy + \frac{3}{2}\frac{U}{R}\sin\theta\frac{\partial}{\partial\theta}\int_0^{\delta}\phi dy \tag{7}$$

where ϕ is the dimensionless temperature ratio, $\phi = \frac{T - T_\infty}{T_i - T_\infty}$

Assuming the boundary condition, $\frac{\partial\phi}{\partial y} = 0$ at $y = \delta$

The left hand side of Eq. (7) becomes

$$\alpha\int_0^{\delta}\frac{\partial^2\phi}{\partial y^2}dy = \alpha\frac{\partial\phi}{\partial y}\bigg|_0^{\delta} = -\alpha\left(\frac{\partial\phi}{\partial y}\right)_{y=0} \tag{8}$$

And Eq. (7) is expressed as

$$-\alpha\left(\frac{\partial\phi}{\partial y}\right)_{y=0} = -\left(3\frac{U}{R}\cos\theta + 2\frac{\dot{R}}{R}\right)\int_0^{\delta} y\frac{\partial\phi}{\partial y}dy + \frac{3}{2}\frac{U}{R}\sin\theta\frac{\partial}{\partial\theta}\int_0^{\delta}\phi dy \tag{9}$$

If ϕ is taken to be a simple power series in y, Eq. (9) can be simplified further. Here a cubic of the form,

$$\phi = \frac{3}{2}\left(1 - \frac{y}{\delta}\right)^2 - \frac{1}{2}\left(1 - \frac{y}{\delta}\right)^3 \tag{10}$$

is assumed, the boundary conditions $\phi = 1$, $\frac{\partial^2\phi}{\partial y^2} = 0$ at $y = 0$ and $\phi = \frac{\partial\phi}{\partial y} = 0$ at $y = \delta$.

As the temperature at the vapor liquid interface, T_i is constant and equal to the saturation temperature at all points on the bubble surface, $\frac{\partial \phi}{\partial \theta} = 0$

Calculating the terms in Eq. (9) by substituting the value of ϕ, given by Eq. (10),

$$\left(\frac{\partial \phi}{\partial y}\right)_{y=0} = -\frac{3}{2\delta} \quad ; \quad \int_0^{\delta} y \frac{\partial \phi}{\partial y} dy = -\frac{3}{8}\delta \quad ; \quad \frac{\partial}{\partial \theta}\int_0^{\delta} \phi dy = \frac{3}{8}\frac{\partial \delta}{\partial \theta} \tag{11}$$

Substitution of Eq. (11) in Eq. (9) gives,

$$\frac{3}{2}\frac{\alpha}{\delta} = \left(2\frac{\dot{R}}{R} + 3\frac{U}{R}\cos\theta\right)\frac{3}{8}\delta + \frac{9}{16}\frac{U}{R}\sin\theta\frac{\partial \delta}{\partial \theta}$$

$$\therefore \frac{1}{2}\frac{\partial \delta^2}{\partial \theta} = \frac{8}{3}\frac{\alpha R}{U\sin\theta} - \frac{2}{3\sin\theta}\left(\frac{2\dot{R}}{U} + 3\cos\theta\right)\delta^2$$

Dividing by R^2 and letting $\varepsilon = \left(\frac{\delta}{R}\right)^2$ and hence $\partial\delta^2 = R^2\partial\varepsilon$,

$$\frac{\partial \varepsilon}{\partial \theta} = -\frac{4}{3}\left(\frac{2\dot{R}}{U} + 3\cos\theta\right)\frac{\varepsilon}{\sin\theta} + \frac{16}{3}\left(\frac{\alpha}{UR}\right)\frac{1}{\sin\theta} \tag{12}$$

This is a first order, first degree, linear differential equation in ε, which can be solved as follows:

$$\frac{\partial \varepsilon}{\partial \theta} + P\varepsilon = Q \tag{13}$$

where $P = \frac{4}{3\sin\theta}\left(\frac{2\dot{R}}{U} + 3\cos\theta\right)$ and $Q = \frac{16}{3}\left(\frac{\alpha}{UR}\right)\frac{1}{\sin\theta}$

The solution for the differential Eq. (13) is given as

$$\varepsilon = e^{-\int P d\theta}\left[\int e^{\int P d\theta} Q d\theta + c\right] \tag{14}$$

Assuming ε = 0 when θ = 0, gives c=0

Substituting the values of P and Q, $e^{-\int P d\theta} = \sin^4\theta\left(\tan\frac{\theta}{2}\right)^{\frac{8}{3}\frac{\dot{R}}{U}}$

Hence, Eq. (14) becomes,

$$\varepsilon = \frac{1}{\sin^4\theta\left(\tan\frac{\theta}{2}\right)^{\frac{8}{3}\frac{\dot{R}}{U}}}\left[\frac{16}{3}\left(\frac{\alpha}{UR}\right)\int_0^{\theta}\sin^3\theta\left(\tan\frac{\theta}{2}\right)^{\frac{8}{3}\frac{\dot{R}}{U}}d\theta\right] \tag{15}$$

$$\frac{\delta}{R} = \frac{4}{\sqrt{3}}\left(\frac{\alpha}{UR}\right)^{1/2}\frac{1}{\sqrt{\sin\theta\ F\left(\theta,\frac{\dot{R}}{U}\right)}}\left[\int_0^{\theta}F\left(\theta,\frac{\dot{R}}{U}\right)d\theta\right] \tag{16}$$

where $F\left(\theta,\frac{\dot{R}}{U}\right) = \left[\sin^3\theta\left(\tan\frac{\theta}{2}\right)^{\frac{8}{3}\frac{\dot{R}}{U}}\right]$

The heat flux at an angular position θ on the surface of the bubble is given as

$$q_\theta = -k\left(\frac{\partial T}{\partial y}\right)_{y=0} = -k\left(\frac{\partial \phi}{\partial y}\right)_{y=0}\Delta T = \frac{3}{2}\frac{k\,\Delta T}{R}\left(\frac{R}{\delta}\right) \tag{17}$$

where q_θ (heat flux at angular position on the surface of the bubble) in W/m^2, (δ / R) is given by Eq. (16), ΔT (subcooling of water relative to steam) in K and $\Delta T = T_i - T_\infty$.

For the simple case of $\frac{\dot{R}}{U} = 0$, Eq. (18) can be calculated as follows:

$$F(\theta, 0) = \sin^3\theta \tag{18}$$

$$\left[\int_0^{\theta}F(\theta,0)\,d\theta\right]^{1/2} = \left[\frac{\cos^3\theta}{3} - \cos\theta + \frac{2}{3}\right]^{1/2} \tag{19}$$

Substituting the value of $\frac{\delta}{R}\left(\text{with } \frac{\dot{R}}{U} = 0\right)$ from Eq. (16) in Eq. (17) gives,

$$q_\theta = \frac{\rho_l c_p \Delta T\left(\frac{3}{2}\right)\alpha UR\sin^2\theta}{\sqrt{\frac{16}{3}\alpha UR^3\left(\frac{2}{3}\cos\theta + \frac{1}{3}\cos^3\theta\right)}} \tag{20}$$

which is the same form as the exact solution of Ruckenstein [13] but gives a value 6% lower than his solution where c_p (specific heat) in J/kg K and ρ_l (density of liquid) in kg/m^3.

An energy balance on the steam bubble states that the total heat transferred from the bubble at time t is given as

$$Q = \int_0^{\pi} 2\pi R^2 \sin\theta q_0 d\theta = -h_{fg}\rho_v \frac{dV}{dt} \tag{21}$$

where $\frac{dV}{dt}$ is the rate of change of volume of the bubble, Q (rate of heat transfer from the bubble at time t) in W, ρ_v (density of vapour) in kg/m^3 and h_{fg} (specific enthalpy of evaporation) in J/kg.

Substitution of the value of $\left(\frac{R}{\delta}\right)\left(\text{where } \frac{\dot{R}}{U} \neq 0\right)$ from Eq. (16) in (17) gives,

$$q_\theta = \frac{3\sqrt{3}}{8}\frac{k\Delta T}{R}\left(\frac{UR}{\alpha}\right)^{1/2} \frac{\left[\sin\theta F\left(\theta, \frac{\dot{R}}{U}\right)\right]^{1/2}}{\left[\int_0^{\theta} F\left(\theta, \frac{\dot{R}}{U}\right) d\theta\right]^{1/2}} \tag{22}$$

where k (thermal conductivity) in W/m K. This value is then introduced into Eq. (21) to give,

$$-\frac{dV}{dt} = \frac{3\sqrt{6}}{8}\left(\frac{c_p \Delta T \rho_f}{h_{fg}\rho_v}\right)\left(\frac{2UR}{\alpha}\right)^{1/2} \pi R\alpha \int_0^{\pi} \frac{\left[\sin^3\theta\, F\left(\theta, \frac{\dot{R}}{U}\right)\right]^{1/2}}{\left[\int_0^{\theta} F\left(\theta, \frac{\dot{R}}{U}\right) d\theta\right]^{1/2}} d\theta \tag{23}$$

The rate of change of bubble volume is expressed as

$$-\frac{dV}{dt} = -\frac{d}{dt}\left(\frac{4}{3}\pi R^3\right) = -4\pi R^2 \dot{R} = -4\pi R_0^3 \dot{\beta}\beta^2 \tag{24}$$

where R_0 (initial bubble radius) in m and the dimensionless radius, $\beta = \frac{R}{R_0}$.

Introducing the Fourier number, $Fo = \frac{\alpha t}{4R_0^2}$ and substituting $\frac{d\beta}{dt} = \frac{d\beta}{dFo}\frac{\alpha}{4R_0^2}$ in Eq. (24) gives,

$$-\frac{dV}{dt} = -\pi R_0 \beta^2 \alpha \frac{d\beta}{dFo} \tag{25}$$

Thus Eq. (23) can be arranged to give,

$$\beta^{1/2}\frac{d\beta}{dFo} = -\frac{9}{4\sqrt{6}}\,Ja\,Pe_0^{1/2}\int_0^{\pi}\frac{\left[\sin^3\theta\,F\left(\theta,\frac{\dot{R}}{U}\right)\right]^{1/2}}{\left[\int_0^{\theta}F\left(\theta,\frac{\dot{R}}{U}\right)d\theta\right]^{1/2}}d\theta \tag{26}$$

Also,
$$\frac{\dot{R}}{U} = \frac{R_0}{U}\frac{d\beta}{dt} = \frac{R_0}{U}\frac{\alpha}{4R_0^2}\frac{d\beta}{dFo} = \frac{1}{2}\left(\frac{\alpha}{2UR_0}\right)\frac{d\beta}{dFo}$$

$$\therefore \frac{\dot{R}}{U} = \frac{1}{2Pe_0}\frac{d\beta}{dFo} \tag{27}$$

Eqs. (26) and (27) can be combined to give β in terms of $\frac{\dot{R}}{U}$ with Ja (Jakob number) and Pe_0 (Peclet number) as parameters, viz., (The Jakob number describes the ratio of heat which can be stored in the unit of volume of the subcooled liquid until heating it up to saturation temperature to the latent heat of evaporation stored in the unit of volume of the vapor. the Peclet number is a dimensionless number relating the rate of advection of a flow to its rate of diffusion, often thermal diffusion. It is equivalent to the product of the Reynolds number with the Prandtl number in the case of thermal diffusion)

$$\beta = \left[-\frac{9}{8\sqrt{6}}\left(\frac{Ja}{Pe_0^{1/2}}\right)\left(\frac{1}{\dot{R}/U}\right)\int_0^{\pi}\frac{\left[\sin^3\theta\,F\left(\theta,\frac{\dot{R}}{U}\right)\right]^{1/2}}{\left[\int_0^{\theta}F\left(\theta,\frac{\dot{R}}{U}\right)\right]^{1/2}}\right]^2 \tag{28}$$

A typical plot of $\left(-\frac{U}{\dot{R}}\right)$ versus β is shown in Fig. 3 for Ja=15 and $Pe_0=10^4$.

Eq. (27) can be written as

$$Fo_i = \frac{1}{2Pe_0}\int_{\beta_i}^{1}\left(-\frac{U}{\dot{R}}\right)d\beta \tag{29}$$

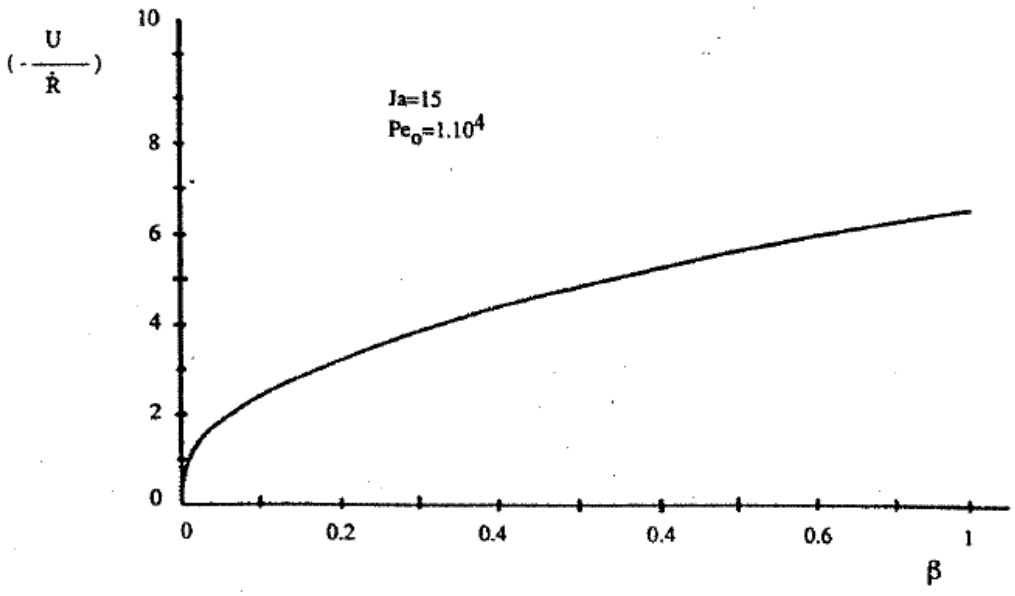


Fig.3. A typical plot of $\left(-\frac{U}{\dot{R}}\right)$ versus β according to equation (28).

Thus, when the curve in Fig. 3 is integrated the corresponding values of Fo_i and β_i can be found, and plotted as shown in Fig. 4. Eq. (26) can be written as

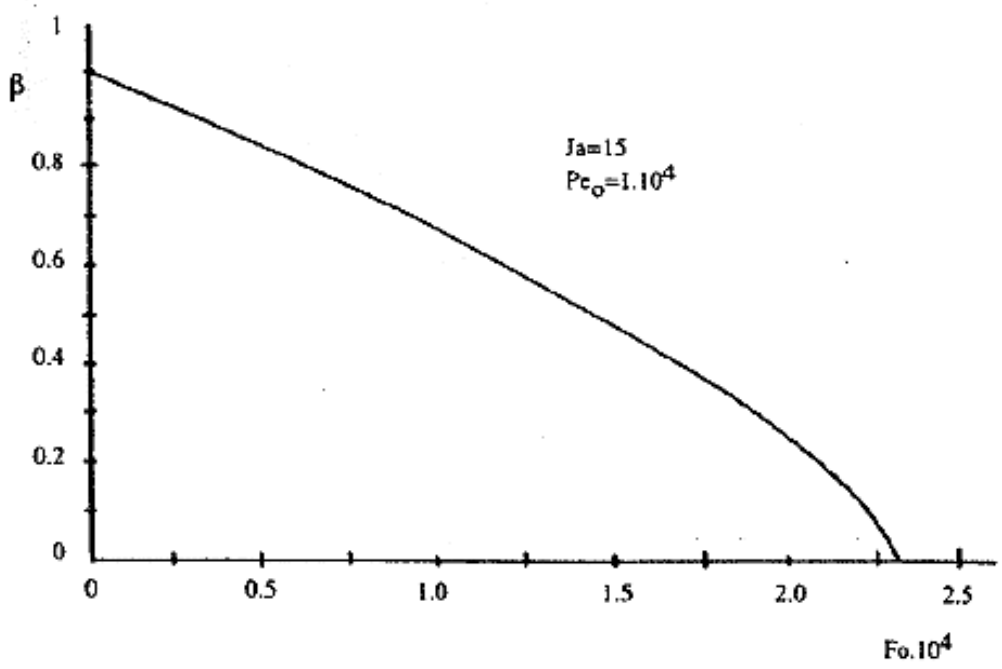


Fig.4. β versus Fo according to equation (29).

$$\beta^{1/2}\frac{d\beta}{dFo} = -\frac{9}{4\sqrt{6}}\,Ja\,Pe_0^{1/2}F_1\left(\frac{\dot{R}}{U}\right) \tag{30}$$

where

$$F_1\left(\frac{\dot{R}}{U}\right) = \int_0^{\pi}\frac{\left[\sin^3\theta\; F\left(\theta,\frac{\dot{R}}{U}\right)\right]^{1/2}}{\left[\int_0^{\theta}F\left(\theta,\frac{\dot{R}}{U}\right)d\theta\right]^{1/2}}d\theta$$

An evaluation of $F_1\left(\frac{\dot{R}}{U}\right)$ versus $\left(\frac{\dot{R}}{U}\right)$ presented in Fig. 5, gives the relationship as

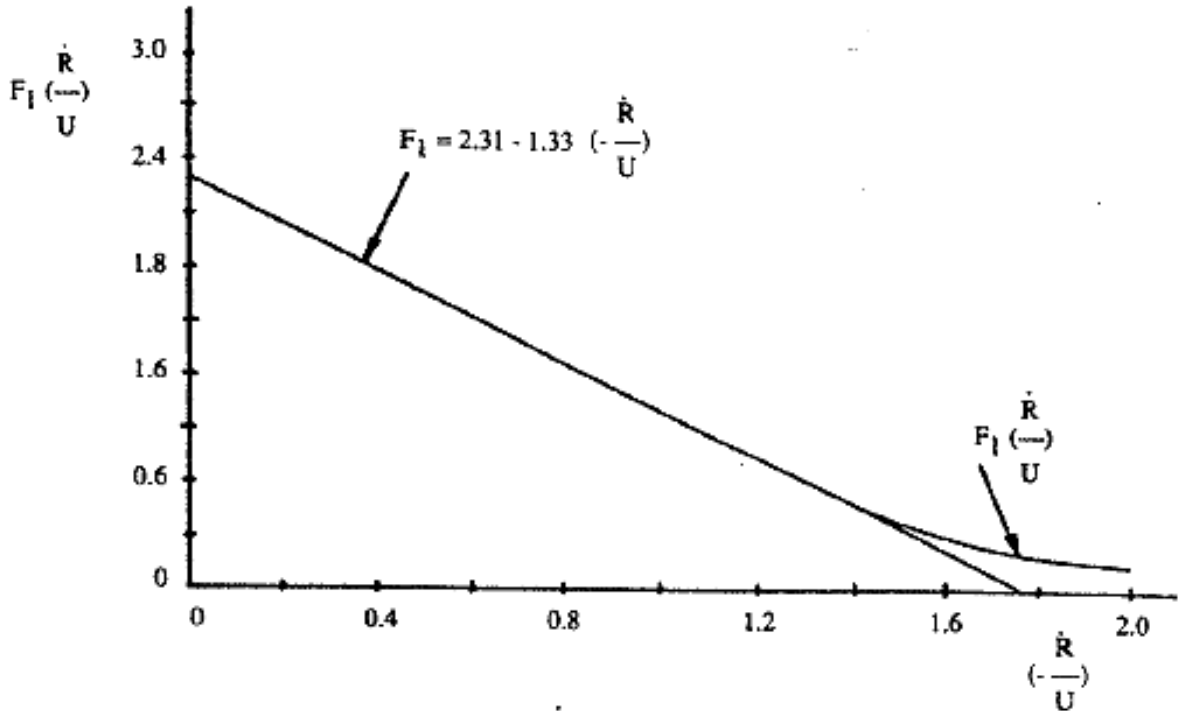


Fig.5. $F_1\left(\frac{\dot{R}}{U}\right)$ versus $\left(-\frac{\dot{R}}{U}\right)$.

$$F_1 \cong 2.31 - 1.33\left(-\frac{\dot{R}}{U}\right) \quad \text{for } 0 \le -\frac{\dot{R}}{U} \le 1.4 \tag{31}$$

Hence Eq. (30) becomes

$$\frac{2}{3}\frac{d\beta^{3/2}}{dFo} = -\frac{9}{4\sqrt{6}} Ja\ Pe_0^{1/2}\left(2.31+1.33\left(\frac{\dot{R}}{U}\right)\right) \tag{32}$$

Substituting $\frac{\dot{R}}{U} = \frac{1}{2Pe_0}\frac{d\beta}{dFo}$ from Eq. (27)

$$\frac{2}{3}\frac{d\beta^{3/2}}{dFo} = -\frac{9}{4\sqrt{6}} Ja\ Pe_0^{1/2}\left(2.31+\frac{1.33}{2Pe_0}\frac{d\beta}{dFo}\right) \tag{33}$$

and integrating gives

$$\left(1-\beta^{3/2}\right) = 3.182Ja\ Pe_0^{1/2}\left[Fo-\frac{0.288}{Pe_0}(1-\beta)\right] \tag{34}$$

Hence, the simplified form of Eq. (28) can be expressed as

$$\beta = \left[1-3.182Ja\ Pe_0^{1/2}\left[Fo-\frac{0.288}{Pe_0}(1-\beta)\right]\right]^{2/3} \tag{35}$$

A comparison of the curve according to the complete Eqs. (28) and (29) calculated by a computer simulation program with the curve according to the simplified Eq. (35) is given in Fig. 6 for Ja=15 and $Pe_0=10^4$. The collapse Fourier number according to the simplified equation is about 2.5% higher than that from Eqs. (28) and (29).

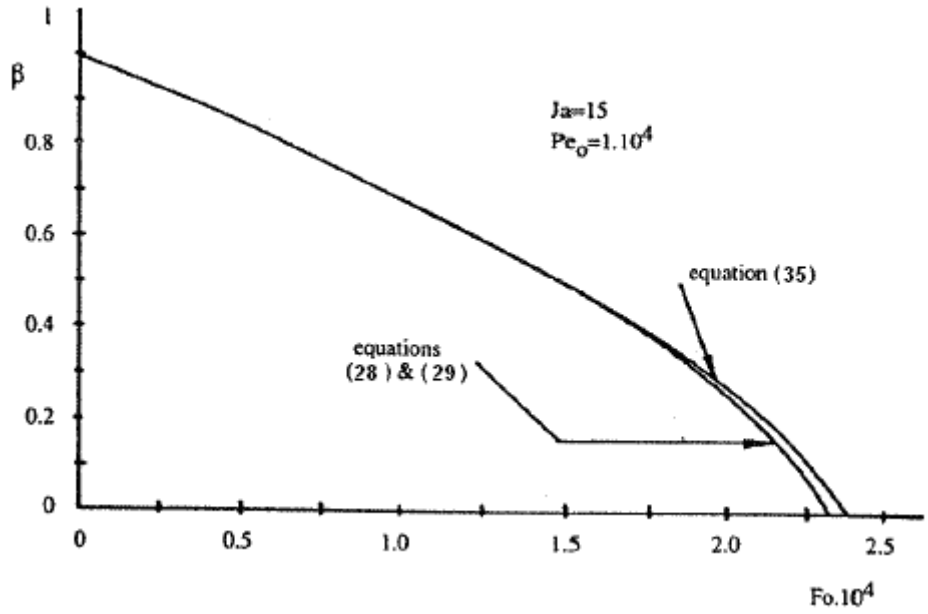


Fig. 6. Comparison of complete and simplified solution.

The collapse Fourier number for the simplified theory in Eq. (35) is given by

$$\mathrm{Fo_c} = \frac{1}{3.182\,\mathrm{Ja}\,\mathrm{Pe}^{1/2}} + \frac{0.288}{\mathrm{Pe_0}} \tag{36}$$

As can be seen from the impressions of bubble shapes in Fig. 7 and Fig. 8, the bubbles were generally far from spherical and indeed changed in shape, sometimes in an oscillating manner, after detachment [14].

The equivalent bubble radius, R was calculated as the radius of a sphere of volume equal to the measured bubble volume V_B. This radius was used in the heat transfer calculations in Eq. (21).

To account for the non-spherical shape of the bubble a shape factor, ψ (bubble shape factor) defined as

$$\psi = \frac{\text{measured bubble surface area}}{4\,\pi\,\mathrm{R}^2} \tag{37}$$

was included in Eq. (21) to give

$$\mathrm{Q} = \left[\int_0^{\pi} 2\pi \mathrm{R}^2 \sin\theta\, \mathrm{q}_\theta\right]\psi \tag{38}$$

Assuming $\psi = \psi(\beta)$, the simplified equation for the bubble collapse rate is now obtained from Eq. (38) as

$$\beta^{1/2}\frac{\mathrm{d}\beta}{\mathrm{dFo}} = -\frac{9}{4\sqrt{6}}\,\mathrm{Ja}\;\mathrm{Pe}_0^{1/2}\psi(\beta)\,\mathrm{F_1}\left(\frac{\dot{\mathrm{R}}}{\mathrm{U}}\right) \tag{39}$$

Substituting the approximate expression, given in Eq. (31), for $\mathrm{F_1}\left(\frac{\dot{\mathrm{R}}}{\mathrm{U}}\right)$ together with the value of $\left(\frac{\dot{\mathrm{R}}}{\mathrm{U}}\right)$ in Eq. (27), Eq. (39) can be written as

$$\beta^{1/2}\frac{\mathrm{d}\beta}{\mathrm{dFo}} = -\frac{9}{4\sqrt{6}}\,\mathrm{Ja}\;\mathrm{Pe}_0^{1/2}\psi(\beta)\left(2.31 + \frac{1.33}{2\mathrm{Pe_0}}\frac{\mathrm{d}\beta}{\mathrm{dFo}}\right) \tag{40}$$

Hence,

$$\int_1^{\beta}\frac{\beta^{1/2}}{\psi(\beta)}\mathrm{d}\beta = -2.122\mathrm{Ja}\;\mathrm{Pe}_0^{1/2}\left[\mathrm{Fo} - \frac{0.288}{\mathrm{Pe_0}}(1-\beta)\right] \tag{41}$$

In the case of $\psi(\beta)$ = constant, Eq. (41) gives

$$\beta = \left[1 - 3.182\,\mathrm{Ja}\;\mathrm{Pe}_0^{1/2}\psi\left[\mathrm{Fo} - \frac{0.288}{\mathrm{Pe_0}}(1-\beta)\right]\right]^{2/3} \tag{42}$$

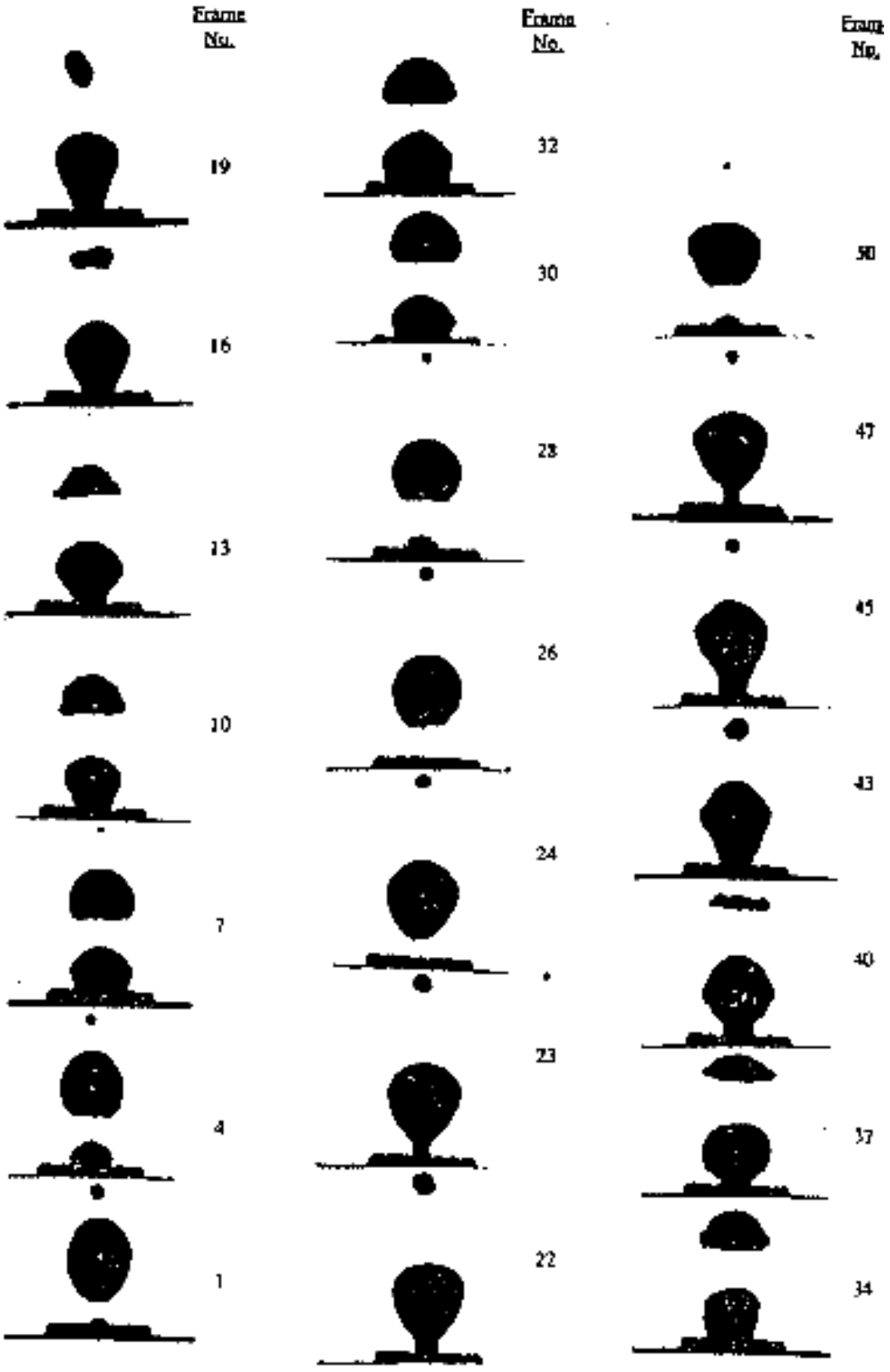


Fig.7. Photographs of bubble growth and collapse.
Ja = 30, Pe_o = 10000, Δt / Frame = 0.79 ms , * Detachment point

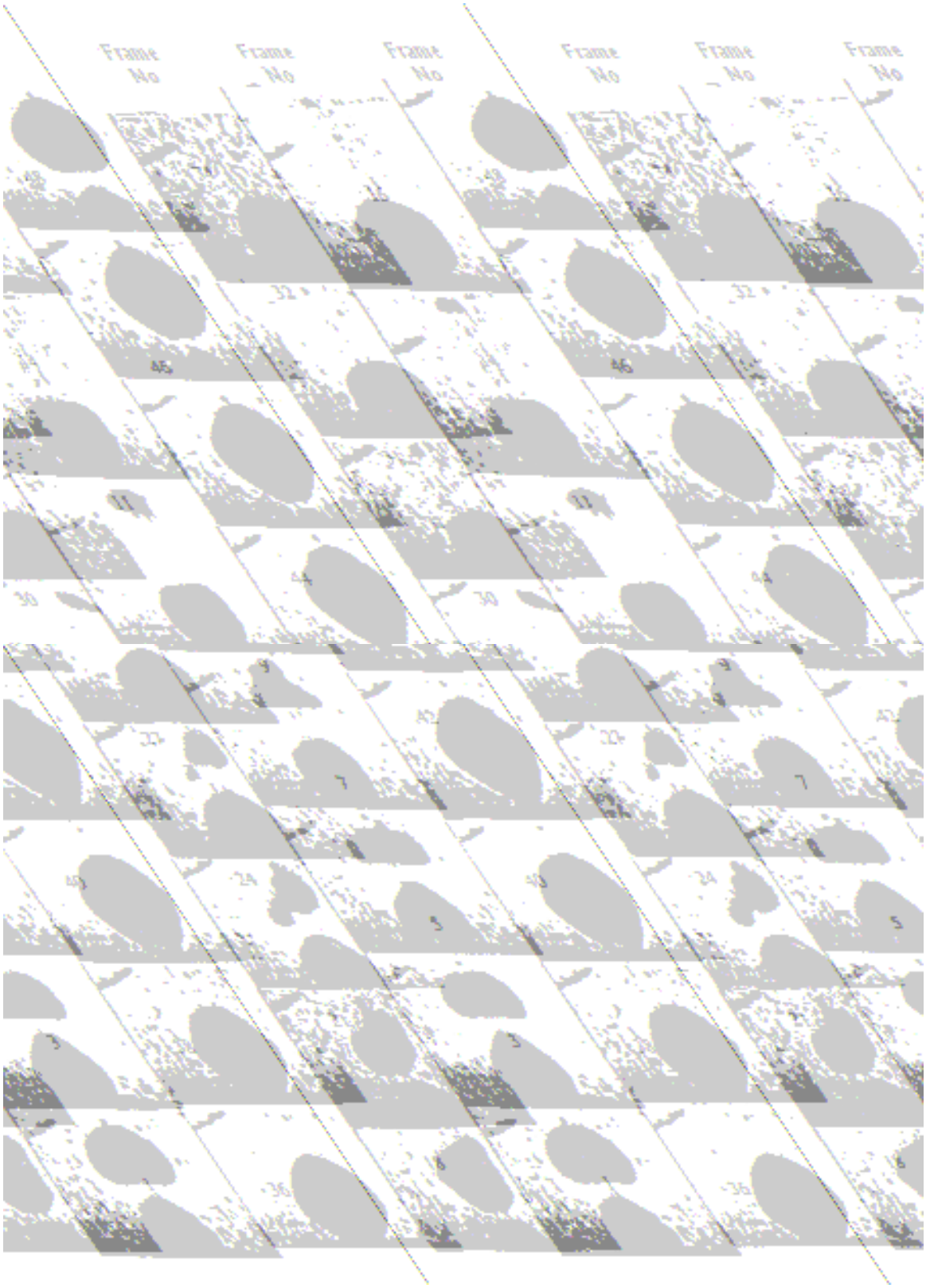


Fig.8. Photographs of bubble growth and collapse.
Ja = 15, Pe_o = 7400, Δt / Frame = 1.186 ms
* Detachment point

Examination of the bubble volume and equivalent radius versus time curves [14] showed that there was significant condensation of the bubble before detachment from the orifice. Therefore, it was assumed that the condensation of the predetached bubble heated the liquid close to the orifice, so that after detachment the bubble rose through liquid where the temperature difference, $\Delta T'$ between the steam and the surrounding water rose from zero to ΔT, the nominal value, according to the simple expression,

$$\frac{\Delta T'}{\Delta T} = \frac{Ja'}{Ja} = \left(\frac{Z}{Z_c}\right)^n = \left(\frac{Fo}{Fo_c}\right)^n \tag{43}$$

where Z_c and Fo_c are the collapse height and collapse Fourier number respectively. It is expected that the index n will be between zero (no heating) and 1 (plane heating) and can be used as an adjustable parameter.

In the case of ψ = constant and negligible bubble wall velocity $\left(\dot{R} = 0\right)$, simplified Eq. (40) for the bubble collapse rate can now be written as

$$-\frac{2}{3}\frac{d\beta^{3/2}}{dFo} = -2.122\ \psi\ Ja'\ Pe_0^{1/2} \tag{44}$$

Substituting $Ja' = Ja\left(\frac{Fo}{Fo_c}\right)^n$ from Eq. (43) and integrating gives,

$$1-\beta^{3/2} = \frac{3.182\,\psi\,Ja\,Pe_0^{1/2}}{n+1}\frac{Fo^{n+1}}{Fo_c^n} \tag{45}$$

The collapse Fourier number, $Fo_c = Fo$ at $\beta = 0$, is

$$Fo_c = \frac{n+1}{3.182\ \psi\ Ja\ Pe_0^{1/2}} \tag{46}$$

Thus, Eq. (45) can be written as

$$\left(1-\beta^{3/2}\right) = \left(\frac{3.182\,\psi}{n+1}\right)^{n+1} Ja^{n+1}\, Pe_0^{\frac{n+1}{2}}\, Fo^{n+1} \tag{47}$$

where a value of n can be chosen to suit the experimental conditions.

5. Comparison of theory with experimental data

Study of the radius ratio versus Fourier number curves [14] suggested that the shape curve could well be followed if n = 0.1 in Eq. (47), thus reducing that equation to the form,

$$\left(1-\beta^{3/2}\right)=\left(\frac{3.182\,\psi}{1.1}\right)^{1.1} \mathrm{Ja}^{1.1}\,\mathrm{Pe}_0^{0.55}\,\mathrm{Fo}^{1.1} \tag{48}$$

A plot of all experimental data in the form of $\beta^{3/2}$ versus $\mathrm{Ja}^{1.1}\,\mathrm{Pe}_0^{0.55}\,\mathrm{Fo}^{1.1}$ is shown in **Fig. 9**.

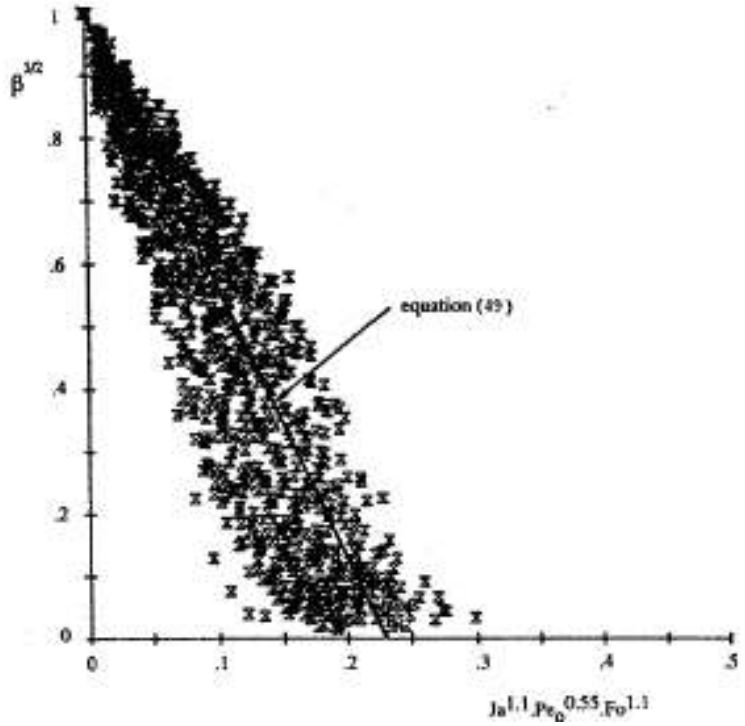


Fig. 9. Plot of all the experimental data [12].

The equation,

$$\left(1-\beta^{3/2}\right)=4.35\,\mathrm{Ja}^{1.1}\,\mathrm{Pe}_0^{0.55}\,\mathrm{Fo}^{1.1} \tag{49}$$

fits the 1134 experimental points with a percentage standard deviation, S_1 of 27.5% of the X coordinate calculated as

$$S_1=\sqrt{\frac{\sum_{i=1}^{N}\left[\left(F-X_i\right)/F\right]^2}{N}}\,x\,100\% \tag{50}$$

where X_i is data point given by $\mathrm{Ja}^{1.1}\,\mathrm{Pe}_0^{0.55}\,\mathrm{Fo}^{1.1}$ for any particular value $\beta^{3/2}$ and F is the corresponding parameter determined by Eq. (49).

The standard deviation defined as

$$S_2 = \sqrt{\frac{\sum_{i=1}^{N}\left[\left(F - X_i\right)\right]^2}{N}} \tag{51}$$

is calculated to be 0.0285.

From Eq. (49), the value of X at the end of bubble collapse is given as

$$X_0 = Ja^{1.1} Pe_0^{0.55} Fo_c^{1.1} = \frac{1}{4.35} \cong 0.23 \tag{52}$$

Thus, a percentage standard deviation related to the collapse Fourier number is found as

$$\frac{S_2}{X_0} 100 = 12.4\% \tag{53}$$

Since $4.35 = \left(\frac{3.182\,\psi}{1.1}\right)^{1.1}$, coefficient 4.35 implies a shape factor, ψ of 1.316, about 16% higher than the average of the shape factors (ψ_m = 1.134) [14].

In Figs. 10, 11 and 12, the experimental data plotted individually for some tests as radius ratio (β) versus Fourier number (Fo) are compared with Eq. (49). (Experimental data of three bubbles for each condition are shown with three different symbols in these figures: *, +, ⧖) The plots indicate that Eq. (49) gives a fairly accurate prediction of the collapse.

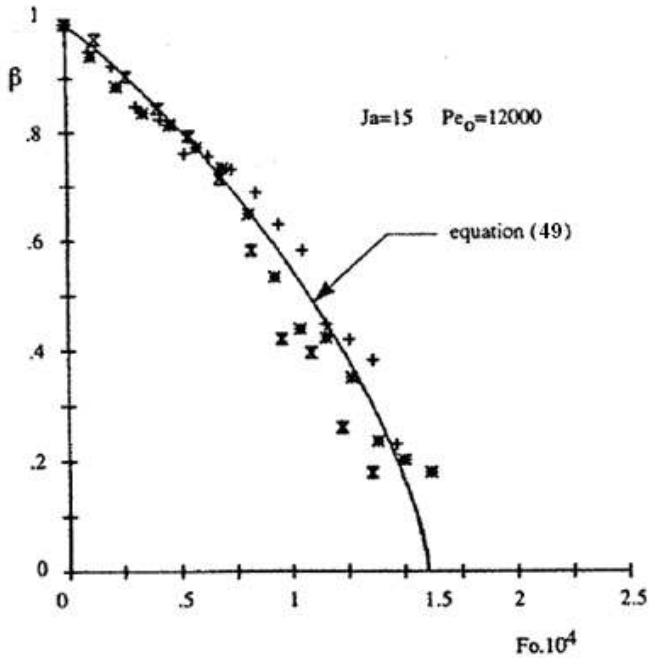


Fig.10. Radius ratio versus Fourier number.

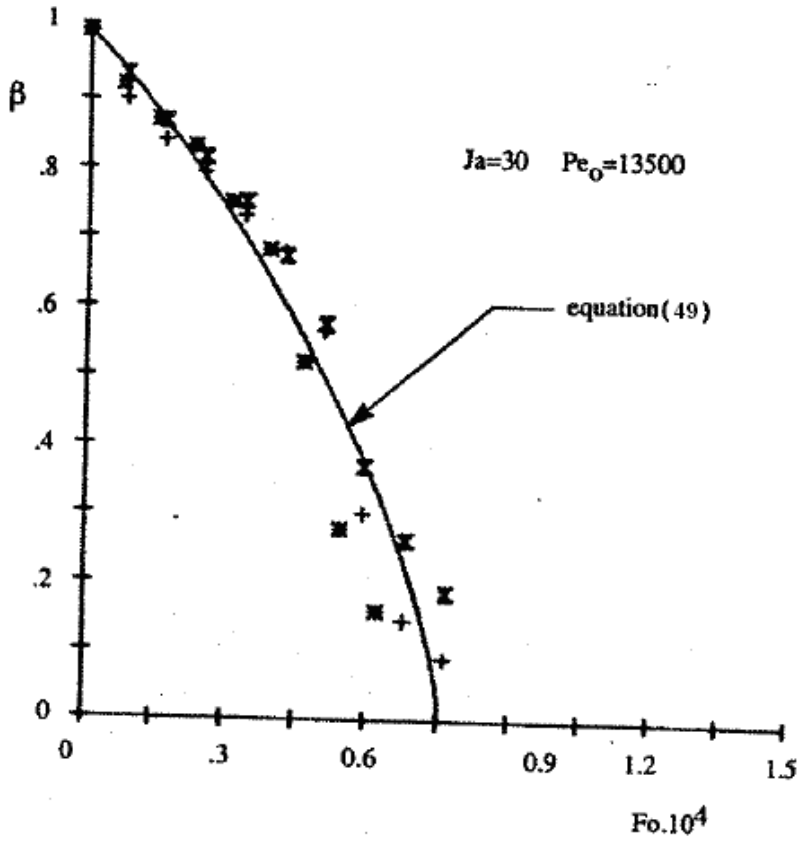


Fig.11. Radius ratio versus Fourier number.

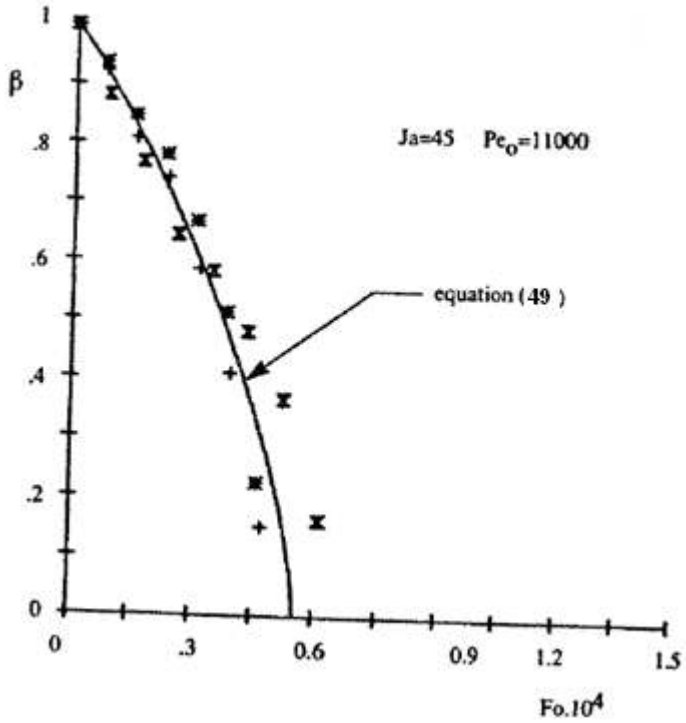


Fig.12. Radius ratio versus Fourier number.

6. Conclusions

The condensation process of steam bubbles injected through an orifice is quite complicated, since bubbles are distorted to some extent. Also the heating of the water, close to the orifice, caused by the condensing bubbles, introduces changes in the experimental conditions around the emerging and condensing bubbles.

The semi-empirical Eq. (49), which considers both bubble distortion and the heating of the liquid around the condensing bubble, correlates the experimental data reasonably well.

Cooling carried out by means of the latent heat of ice will save on electrical energy. It will be possible to use an existing cooling system as a heating system in the winter, so that fuel will be saved on the one hand and pollution will be reduced in the other hand. Furthermore, the system's water content can be used as utility water after cooling by means of ice balls (capsules) made of snow [15-17].

References

[1] Bankoff SG. Diffusion-controlled bubble growth. Adv Chem Eng 1966;6:1-60.
[2] Van Stralen SJD, Cole R. Boiling Phenomena, Hemisphere Publishing Corporation, 1979.
[3] F. Kreith and R. Boehm, Direct Contact Heat Transfer, Hemisphere, New York, 1987.
[4] Kalman H, Mori YH. Experimental analysis of a single vapour bubble condensing in subcooled liquid. Chem Eng J 2002;85:197–206.
[5] Ruckenstein E, Davis EJ. The effects of bubble translation on vapour bubble growth in a superheated liquid. Int J Heat Mass Transfer 1971;14:939-952.
[6] Mayinger F. Heat transfer at the phase interface of bubbles collapsing in subcooled liquids and during subcooled boiling. Heat Mass Transfer 2006;42:869–874.
[7] Florschuetz LW, Chao BT. On the mechanics of vapor bubble collapse. ASME J Heat Transfer 1965;87:209–220.
[8] Isenberg J, Sideman S. Direct contact heat transfer with change of phase: bubble condensation in immiscible liquid. Int J Heat Mass Transfer 1970;13:997–1011.
[9] Jacobs HR, Fannar H, Beggs GC. Collapse of bubble of vapor in immiscible liquid. Proceedings of the Sixth International Heat Transfer Conference 1978;2:383–388.
[10] Kamei S, Hirata M. Study on condensation of a single vapor bubble into subcooled water, Part 2-experimental analysis. Heat Transfer Jpn Res 1990;19:1–10.
[11] Isikan MO. Condensation of spherical-cap shaped bubbles. Int J Heat Mass Transfer 1990;33:1099–1103.
[12] Zeitoun O, Shoukri M, Chatoorgoon V. Interfacial heat transfer between steam bubbles and subcooled water in vertical upward flow. J Heat Transfer 1995;117:402–407.
[13] Ruckenstein E. On heat transfer between vapour bubbles in motion and the boiling fluid from which they are generated. Chem Eng Sci 1959;10:22-30.
[14] Isıkan MO. Colapse of steam bubbles in subcooled water, PhD. Thesis, University of Strathclyde, Glasgow, 1986.
[15] Cerci Y. Experimental investigation of capacitor effects on performance parameters planning for household refrigerator and energy systems. Energy Educ Sci Technol Part A 2009;24:15-24
[16] Ulusarslan D, Gemici Z, Teke I. Currency of district cooling systems and alternative energy sources. Energy Educ Sci Technol Part A 2009;23:31-53
[17] Gungor C, Kaya D. Experimental investigation of the effect of absorber pre-cooler to the performance of the absorption cooling system. Energy Educ Sci Technol Part A 2009;24:71-83